Supporting Information for

Mitigating intubation stress, mucosa injury, and inflammatory response in nasogastric tube intubation via suppression of NF-κB signaling pathway by engineering hydration lubrication coating

Xi Liao[a,d,1], Meng-Han Bai[b,f,1], Yu-Wei Liu[a], Yu-Qing Wei[b], Jun-Yang Wang[b], Zhi-Guo Wang[a], Rui Hong[a], Ju-Xiang Gou[e], Jia-Zhuang Xu[a,b,*], Zhong-Ming Li[b,c], Ka Li[a,*]

[a] *West China Hospital, Sichuan University/West China School of Nursing, Sichuan University, Chengdu 610041, China*

[b] *College of Polymer Science and Engineering, State Key Laboratory of Polymer Materials Engineering, Sichuan University, Chengdu 610065, China*

[c] *West China Hospital, Sichuan University /West China School of Medicine, Sichuan University, Chengdu 610041, China*

[d] *Department of General Surgery, West China Hospital, Sichuan University / Colorectal Cancer Center, West China Hospital, Sichuan University, Chengdu 610041, China*

[e] *Thyroid Surgery Department, West China Hospital, Sichuan University, Chengdu 610041, China*

[f] *Department of Mechanical Engineering, The University of Hong Kong, Hong Kong SAR 999077, China*

[*] Corresponding authors

E-mail address: lika127@126.com *(K. L.)*

E-mail address: jzxu@scu.edu.cn (J. Z. X.)

[1] These authors contributed equally to the present work.

This PDF file includes:

1. Surface morphology and properties

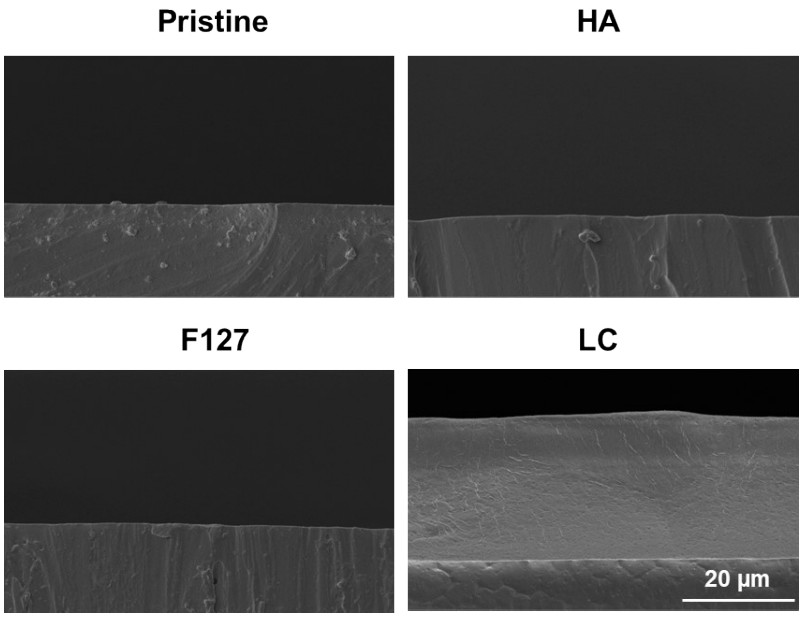

Figure S1. Cross-sectional SEM images of tubes decorated by different coating.

There is almost no coating generated on the only HA-coated and only F127-coated NGT surface. In sharp contrast, the coating with the thickness of ~30μm is formed on the NGT surface. It is not only because of the hydroxyl anchoring sites on the interface, but also is attributed to the strong hydrogen bonding of HA/F127 micelles.

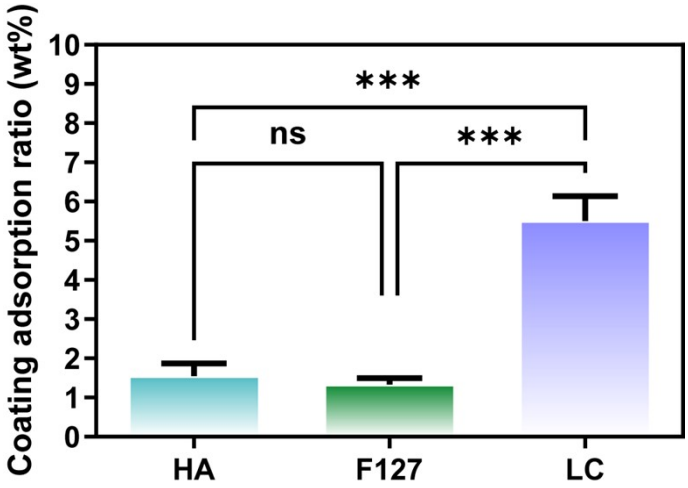

Figure S2. Coating adsorption ratio of the coated tube. Error bars represent ± SD (n = 4).

Coating adsorption ratio was calculated according to the following equation by a gravimetric method:

Coating adsorption ratio = $(W_1\text{-}W_0) / W_0 \times 100\%$

Where W_0 and W_1 represent the dry weight of the original substrate and the coated substrates, respectively.

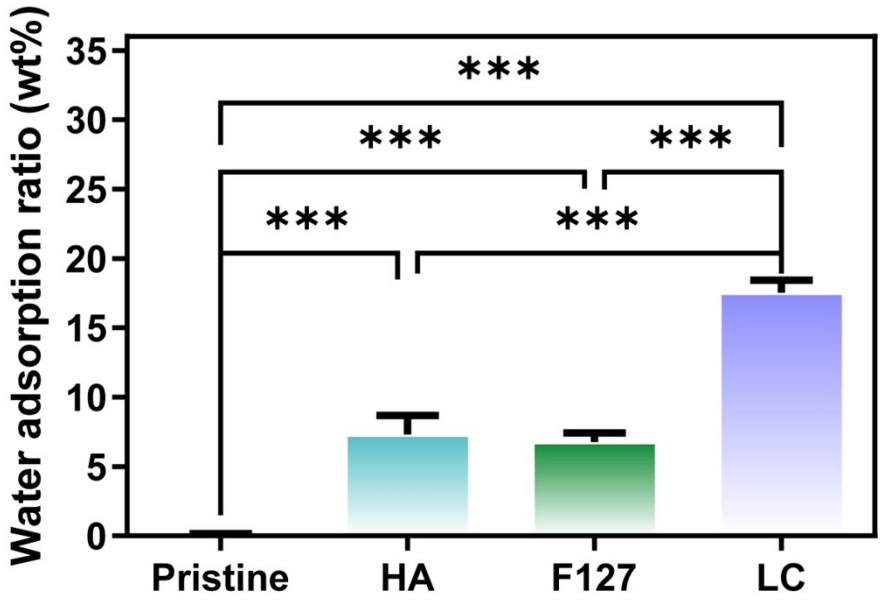

Figure S3. Water adsorption ratio of the coated tube. Error bars represent ± SD (n = 4).

The water adsorption ratio was calculated according to the following equation by a gravimetric method:

Water adsorption ratio = $(W_2\text{-}W_1) / W_0 \times 100\%$

Where W_0, W_1, W_2 represent the weight of the original substrate, the substrates after immobilization and after water absorption, respectively.

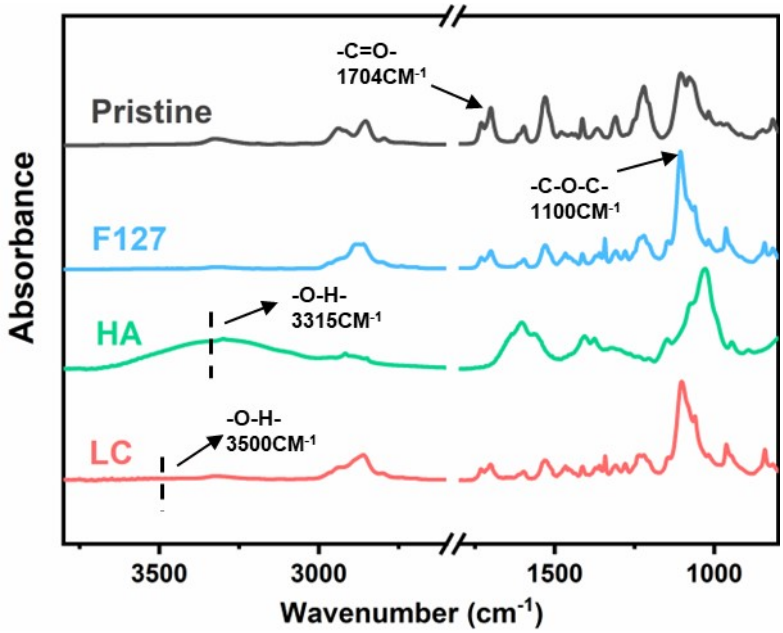

Figure S4. FTIR spectra of the substrates coated by F127, HA, and LC. The appearance of C-O-C stretching vibration and C=O asymmetrical stretching vibration at 1704 and 1103 cm^{-1} confirms the successful application of lubricating coating.

Structural characterization

Figure S4 shows the Fourier transform infrared (FTIR) spectrum of the substrate decorated by the micelle coating. And FTIR spectra of the substrates coated only by HA and F127 are also present for comparison. The peaks at 3324, 1598 and 1704 cm^{-1} are assigned to N-H stretching vibration, N-H bending vibration and C=O stretching vibration, respectively, which are typical characteristic peaks of the substrate (PU). The F127 coating displays the characteristic peak at 1100 cm^{-1} of –C–O–C– stretching vibration and the HA coating shows a peak at 1604 cm^{-1}, which is the C=O asymmetrical stretching vibration of HA. The appearance of C-O-C stretching vibration and C=O asymmetrical stretching vibration at 1604 and 1103 cm-1 confirms the successful formation of the micelle coating. The -OH band displays a redshift

from 3500 to 3315 cm^{-1}, confirming the strong hydrogen bonding between F127 and HA.

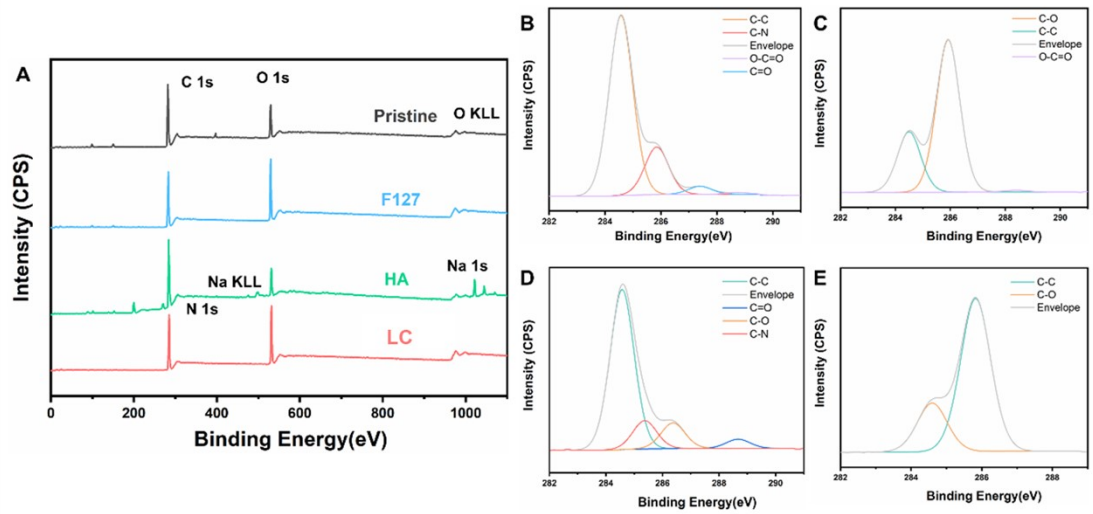

Figure S5. XPS full-spectra and High-resolution spectra of the coated coating. (A)XPS full-spectra of the coated tubes. High-resolution spectra of the C1s peak for (B) the pristine tube, (C) the F127 coated, (D) HA coated, and (E) micelle coated tubes. The XPS wide scans of pristine NGT and LC show the consistent C1s and O1s peaks, while the high-resolution scan shows the multi-peak fitting results of the pristine NGT are replaced by those of the micelle coating.

Water absorption ratio

The water absorption of the coating was measured by the mass change of tubes in DIW for 10 min.

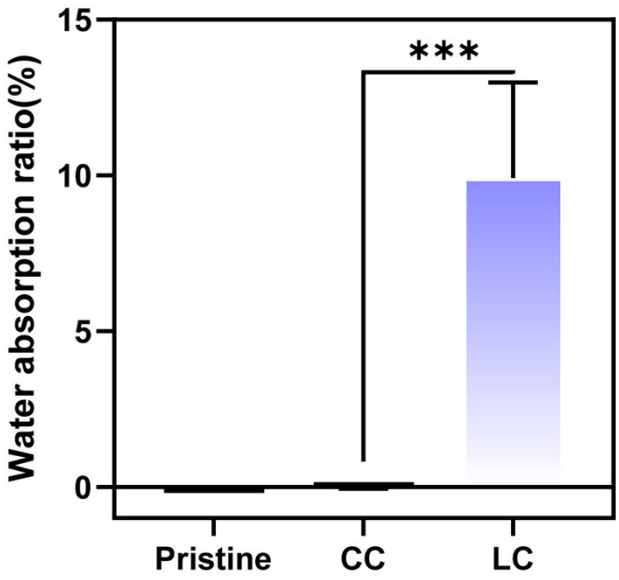

Figure S6. Water adsorption ratio after swelling equilibrium of the coating. Error bars represent ± SD (n = 4). ***p < 0.001, compared to the CC.

High water absorption capacity. The water absorption rates of the samples decorated by different coating were evaluated by the weight change rates (Figure S6). Due to the hydrophobicity of paraffin oil, the water absorption rate of the paraffin oil coating is consistent with that of the pristine substrate. As for the micelle coating, the water absorption rate is 9.9%. The strong hydrogen bond between HA and F127 enables the coating with excellent water retention performance.

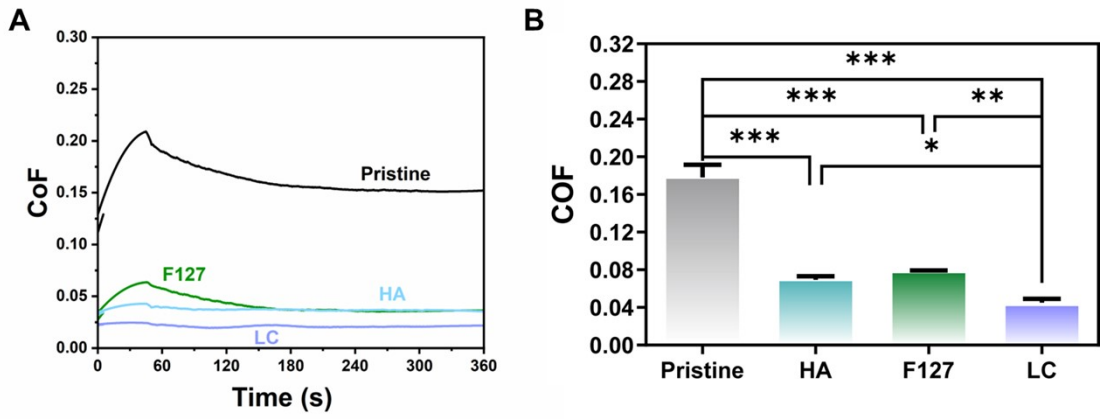

Figure S7. The friction properties of the coated samples. (A) CoF curves for the substrates decorated by different coating as a function of time. (B) The average CoF values of the substrates decorated by different coating. Error bars represent ± SD (n = 3).

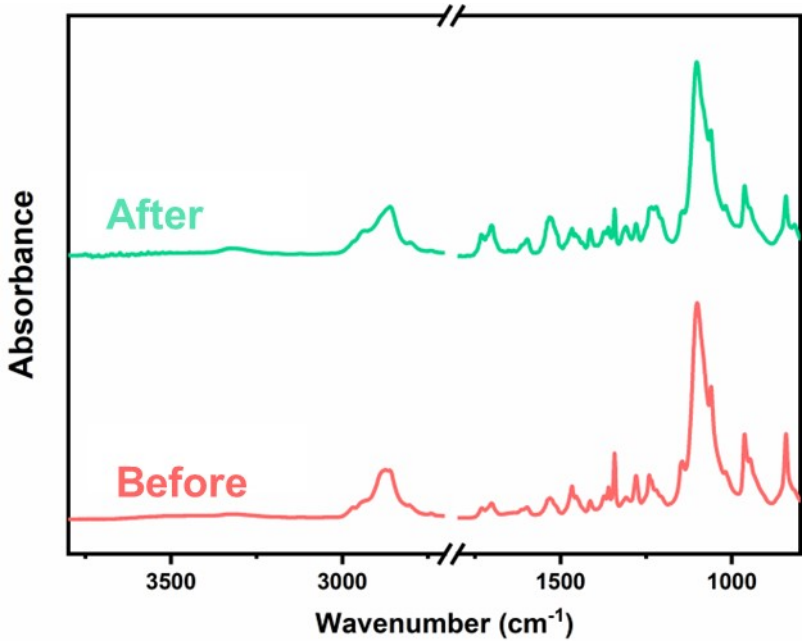

Figure S8. FTIR spectra of LC before and after storage for 3 months. The micelle coating also has good storage stability. The chemical structure of the coating does not change at room temperature for 3 months.

2. Protein adsorption evaluation

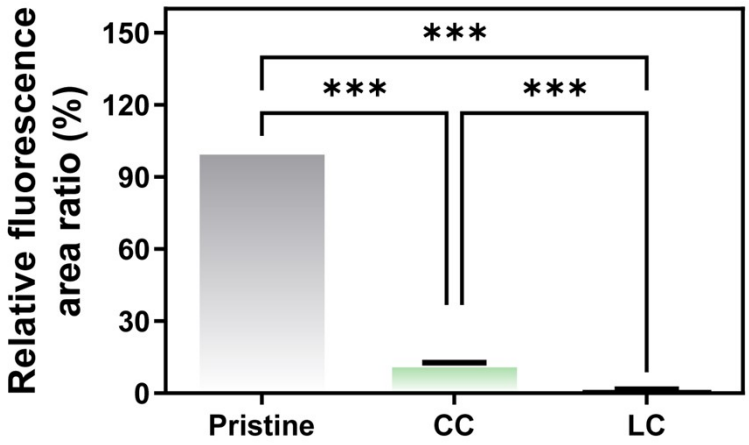

Figure S9. Relative fluorescence area ration for protein fluorescence adsorption experiment. Error bars represent ± SD (n = 3). *p < 0.05, **p < 0.01, and ***p < 0.001. The fluorescence area ratio of the LC group is significantly lower than that of the pristine group and CC group. These data demonstrate that the anti-protein adsorption ability of the micelle coating is superior to the traditional paraffin lubricant coating.

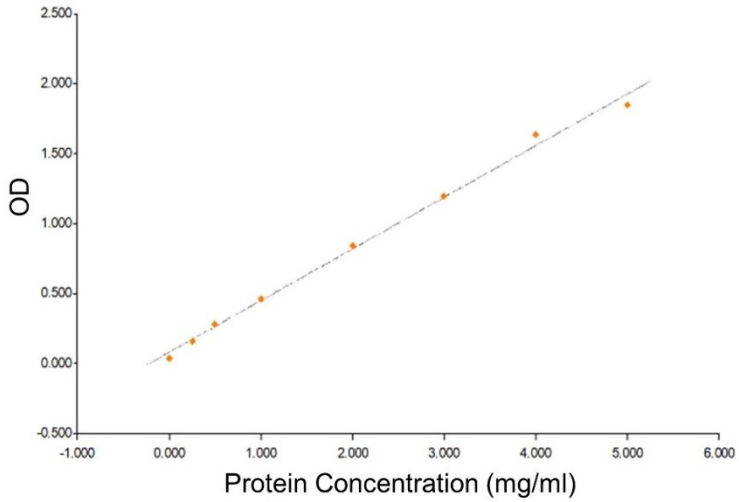

Figure S10. Standard curve for protein adsorption experiments. Y = 0.371x + 0.111 (R_2 = 0.99).

3. *Skin irritation test*

Three healthy adult New Zealand rabbits were used to record the skin integrity stimulation.

Before the experiment, the hair on the back was carefully removed without damaging the skin. Each rabbit was injected with the leach liquor of the coated tubes. As shown in Figure S11, skin was prepared 12 h in advance on both sides of the dorsal spine, followed by intradermal injection performed at 5 injection points (0.2 ml/ point) in each group. Skin reactions including edema and erythema were observed at 20 min, 24 h, 48 h, and 72 h after injection.

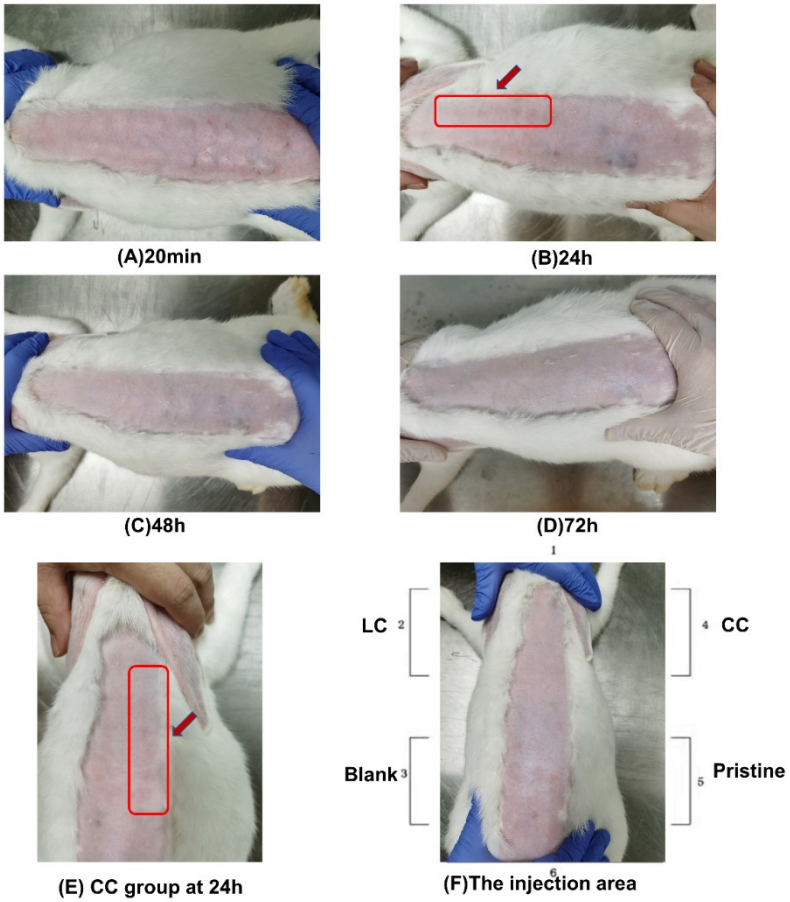

Figure S11. Skin irritation test. Photographs of the back skin injected with the leach liquor of the coated tubes after (A) 20 min, (B) 24 h, (C) 48 h, (D)72 h. (E) The enlarged photograph of (B) to indicate the erythema area (red arrow) of the CC group after injecting the leach liquor for 24 h. The LC group shows no symptoms in the whole period after intradermal injection. (F) The identification of the injected location (1: head, 2: the LC group, 3: the blank group, 4: the CC group, 5: the pristine group, and 6: tail).

***Irritating response of the lubricating coating*:** To evaluate whether the lubricating coating has an irritating response to mucous, erythema and edema symptoms at the injection site of four groups were detected by skin irritation test. As shown in Figure S11E, the CC group shows erythema at the injection area after 24 h intradermal injection, and the LC group shows no symptoms during the whole 72 h after intradermal injection. These results suggest that the micelle coating have better biocompatibility than the paraffin oil coating.

4. Quantitative analysis of mucosal injury

To directly reflect degree of mucosal damage, mucosal injury scoring standard was used to evaluate nasopharyngeal mucosa injury of New Zealand rabbits after nasogastric intubation. Nasopharyngeal mucosa injury is divided into 5 levels (Table S1). In addition, Table S2 was used as the reference to evaluate the damage of nasal mucosa of New Zealand rabbits to quantitatively compare the histopathological changes of different groups.

Table S1. Injury scoring criteria of nasopharyngeal mucosa

Characteristic	Grade/Score	Evaluative criteria
Bleeding and edema	1	Mucosa is normal and smooth without bleeding or edema.
	2	Mucosa is mildly edematous without ulcer or bleeding.
	3	Mucosa is markedly edematous and severely congested.

	4	Mucosa is markedly edematous and hyperemia with sporadic ulcer bleeding.
	5	Mucosa is markedly edematous and hyperemia with large areas of ulcer bleeding.

Table S2. Histopathological scoring criteria of nasal mucosa

Characteristic	Grade/Score	Evaluative criteria
Hyperemia edema	0	No hyperemia edema.
	1	The connective tissue of lamina propria is loose and edematous, and a small number of capillaries are congested and dilated, without exceeding 1/2 of the lamina propria.
	2	The connective tissue of lamina propria is loose and edematous, and many capillaries are congested and dilated, accompanied by more than 1/2 of the lamina propria. But the structure is arranged neatly.
	3	The lamina propria and submucosa are highly loose and edematous, with disordered arrangement and unclear structure. And capillaries are highly dilated and diffusely distributed.
Inflammatory	0	No infiltration.

cell infiltration	1	There is a small amount of inflammatory cell infiltration in the mucosal epithelium and lamina propria with scattered distribution.
	2	There are many inflammatory cell infiltrations in the mucosal epithelium and lamina propria.
	3	A large number of inflammatory cells infiltrated mucosal epithelium and lamina propria, showing a diffuse or multifocal distribution, with obvious inflammatory cell exudation.
Sloughing of mucosal epithelium	0	The mucous membrane is normal without shedding.
	1	A small number of mucosal epithelial cells are degeneration and necrosis, and the shedding of mucosal epithelium is less than 1/2.
	2	Mild degeneration, necrosis and shedding of mucosal epithelial cells, and the shedding of mucosal epithelial cells is more than 1/2.
	3	Mucosal epithelial cells are obviously degenerated, necrotic and shed. There is no complete structure basically.

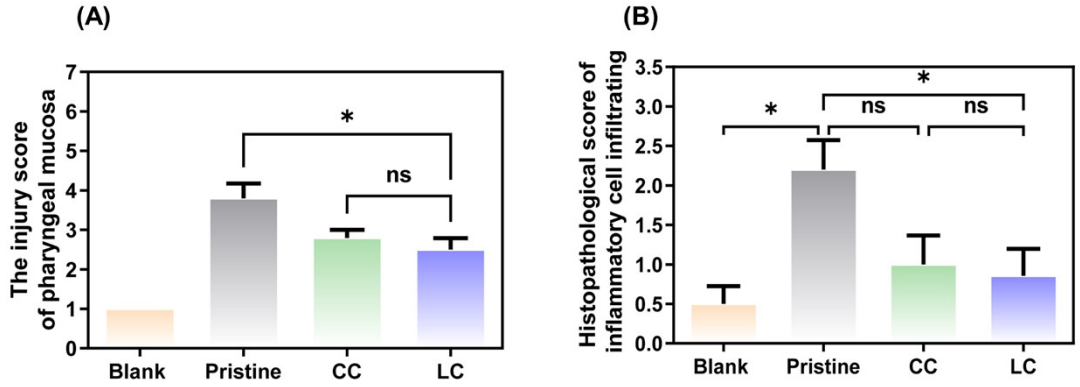

Figure S12. The injury scores and the histopathological score. (A)The injury score of pharyngeal mucosa, Error bars represent ± SD (n = 6). (B) The histopathological score of

inflammatory cells infiltration. Error bars represent ± SD (n = 6). *p < 0.05, **p < 0.01, and ***p < 0.001.

Mucosal injury: The injury score of pharyngeal mucosa in the LC group is significantly lower than in the pristine group (3.80 ± 0.37 vs. 2.50 ± 0.29, p<0.05, Figure S12A）. Meanwhile, the LC group shows a lower histopathological score of inflammatory cells infiltration than the CC group (Figure S12B）.

5.***Effects of the coating on liver and kidney function and immune system***

The concentrations of alanine aminotransferase (ALT), aspartate aminotransferase (AST), creatinine (CREA), and UREA in serum were detected by animal biochemical analyzer (BS-240VET, Shenzhen Mindray Bio-medical Electronics Co., LTD). According to manufacturer's instructions, the concentrations of immunoglobulins (Ig-A, Ig-G and Ig-M, SEA546Rb/ CEA544Rb/ SEA543Rb, Cloud-Clone Corp, China) in the blood were detected by the Elisa experiment.

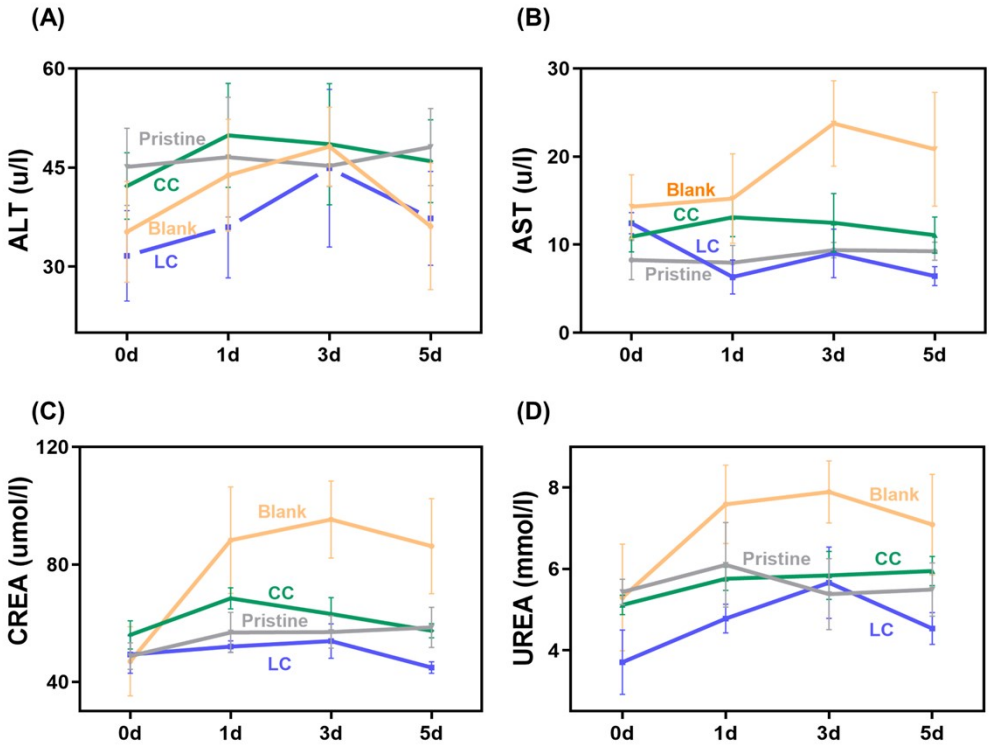

Figure S13. Liver and kidney function indexes. (A)ALT, (B)AST, (C) CREA and (D) UREA on the sixth hour, the third day and fifth day after intubation. Compared with the blank group, there is no abnormal increase for the indexes of liver and kidney function in the LC group. Each point represents the average, error bars represent ± SD (n = 6).

Liver and kidney function indexes: *T*o evaluate the safety of this kind of coating, we assessed the liver and kidney function of body by measuring concentrations of ALT, AST, CREA, and UREA. Compared with the blank group, there is no abnormal increase for the indexes of liver and kidney function in LC group (Figure S13).

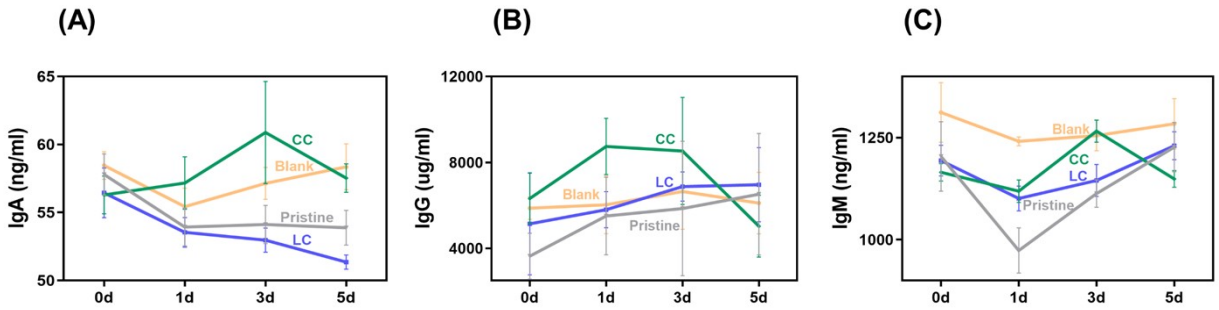

Figure S14. Immune indexes. (A) Ig-A, (B)Ig-G and (C)Ig-M as a function of time after intubation. Compared to the blank group, there is no abnormal increase for these immune indexes in the coated groups. Each point represents the average, error bars represent ± SD (*n* = 6).

Immunoglobulins: We elucidated immune function by measuring immunoglobulin (Ig-A, Ig-G and Ig-M) concentrations on the sixth hour, the third day and fifth day after intubation in the four groups. Ig-A is the main immunoglobulin in mucosal immunity. The low level of Ig-A represents the strengthening of immune function. After being stimulated by specific antigen, Ig-M is produced as the first antibody correlated with the degree of cell damage caused by inflammatory factors. IgG plays a protective role in body's immune system. As shown in Figure S14, compared with the blank group, there is no abnormal increase for these immune indexes in LC group, suggesting that absorption of HA does not affect the immune function of the body.

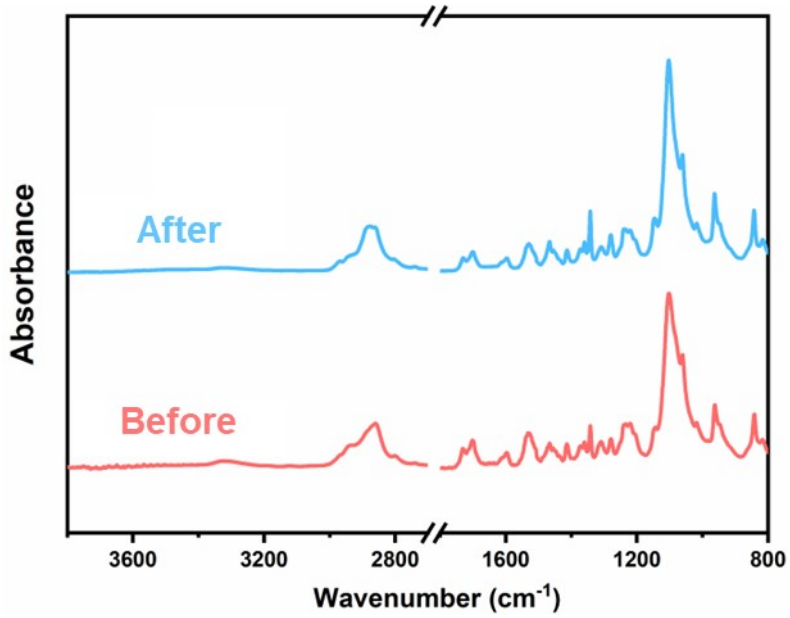

Figure S15. FTIR spectra of LC before and after extubation.

There is almost no change in FTIR spectra of the micelle coated tube before and after extubation, indicating the good stability of the micelle coating.

Table S3. Acronym table**.**

abbreviation	full name	abbreviation	full name
L929	NCTC clone 929	IgA	Immune globulin A
HA	Hyaluronic acid	IgG	Immune globulin G
HAase	Hyaluronidase	IgM	Immune globulin M
CCK-8	Cell Counting Kit-8	ALT	Alanine aminotransferase
α-MEM	MEM Alpha	AST	Aspartate aminotransferase
Elisa	Enzyme-linked immunoas	CREA	Creatinine
WB	Western Blotting	UREA	Carbamide

TLR4	Toll-like receptor 4	PVDF	Poly (vinylidene fluoride)
pIKBα	phospho-IKB alpha	FB	Fibrinogen
pp65	phospho-p65	BSA	Bovine albumin
PBS	Phosphate Buffered Salin	WBC	White blood cell
CRP	C-reactive protein	IL-1β	Interleukin-1β
IL-6	Interleukin-6	TNF-α	Tumor necrosis factor-α